

Electrochemical Machining Multiple Slots of Bipolar Plates with Tool Vibration

Xiaochen Jiang¹, Jia Liu^{1,*}, Ningsong Qu^{1,2}

¹ College of Mechanical and Electrical Engineering, Nanjing University of Aeronautics and Astronautics, Nanjing, China, 210016

² Jiangsu Key Laboratory of Precision and Micro-Manufacturing Technology, Nanjing, China, 210016

*E-mail: meejliu@nuaa.edu.cn

Received: 11 January 2018 / Accepted: 5 April 2018 / Published: 10 May 2018

A bipolar plate is an important component of proton exchange membrane fuel cells (PEMFC). The fabrication of multiple slots is a key part in preparation of metallic bipolar plates. They can be produced by electrochemical machining (ECM). During the ECM process, high flow resistance occurs with the increase of slots length and depth, which will make metal hydroxide and other by-products accumulate in the outlet of electrolyte and limit the maximum feed rate of cathode. Therefore, a flow channels contraction cathode structure with variable cross-section has been proposed. It can make the flow velocity of electrolyte increase gradually in the inter-electrode gap and take away electrolysis products better. In order to remove electrolysis products further, tool vibration is applied. The flow channels contraction cathode has been determined with numerical simulations, and the comparison experimental results show that the way is effective in improving the feed rate and ensuring the uniformity of slots depth.

Keywords: electrochemical machining; bipolar plate; multiple slots; vibration

1. INTRODUCTION

Proton exchange membrane fuel cells (PEMFC) have extensive applications in the portable devices, automotive filed and combined heat and power system. They have been receiving significant attention due to their high power density, energy efficiency, and zero emission compared to traditional power sources. Bipolar plates play an important role in PEMFC. They have traditionally been fabricated from high-density graphite and accounts for most of the weight and volume in a typical fuel cell stack [1]. However, molecular structure of graphite leads to high manufacturing cost, poor mechanical properties and poor efficiency [2]. As a result, metallic bipolar plates have been employed widely because of its excellent mechanical, electrical and thermal properties in recent years [3]. The

fabrication of multiple slots is a key part in preparation of metallic bipolar plates. There are many ways to machine multiple slots of metallic bipolar plates, such as hydroforming [4], stamping [5], and die-casting [6] and so on.

In recent years, electrochemical machining (ECM) has been used in the fabrication of multiple slots of metallic bipolar plates, because it has significant advantages over other machining technologies, such as low production cost, no burr and no tool wear [7]. There are three ways to obtain slots by ECM. The first way is to produce slots one by one. Natsu et al. developed electrolyte jet machining to generate single slot [8]. Chen et al. machined a slot by electrochemical milling with a rotational electrode [9]. Ghoshal et al. electrochemically machined a slot with 1000 μm length and 50 μm depth by micro tool [10]. The second way is through-mask electrochemical micromachining [11]. Nevertheless, the process was complicated and the depth of grooves was low. And the third way is to produce slots by one step, in which the negative mirror image of multiple slots exists in cathode. This is a promising method to prepare multiple slots because of its high efficiency. Lee et al. proposed an electrode to prepare slots with the depth of 200 μm [12]. The increase of slots length and depth is an important aspect in the development of bipolar plates, it is also a challenge to the third way of ECM. During the third way of ECM process, high flow resistance occurs with the increase of slots length and depth, which will make metal hydroxide and other by-products accumulate in the outlet of electrolyte and limit the maximum feed rate of cathode. This could reduce the surface quality and process stability, even worse, a short circuit will happen. To improve the flow field in the third way of ECM process, Zhang et al. designed a multi-functional cathode that filled with elastic blocks [13], and Liu et al. introduced low frequency tool vibrations in ECM [14].

This paper focuses on the fabrication of multiple slots with the length of 60mm in one step by shaped electrode. Based on the feature of flow channels, a flow channels contraction cathode structure with variable cross-section has been proposed, which is used to improve the flow channels and increase feed rate. In order to remove electrolysis products further, tool vibration is also adopted. In this study, the flow field of different shaped cathodes with vibration are simulated and the comparison experiments are also carried out.

2. THE FLOW FIELD ANALYSIS OF MULTIPLE SLOTS

The schematic diagram of electrochemical machining the multiple slots in one step is shown in Fig.1. The workpiece is connected with the positive pole of the power supply. The tool which has rectangular convex array structure is connected with the negative pole of the power supply. The electrolyte flows with high velocity through the inter-electrode gap between cathode and anode. During the ECM processing, the workpiece materials which face and close to the machining surfaces of cathode are dissolved and taken away by flowing electrolyte. The workpiece material face and close to the insulation coatings of cathode are retained. With the tool continuous feeding, the multiple slots on workpiece were performed in one ECM step.

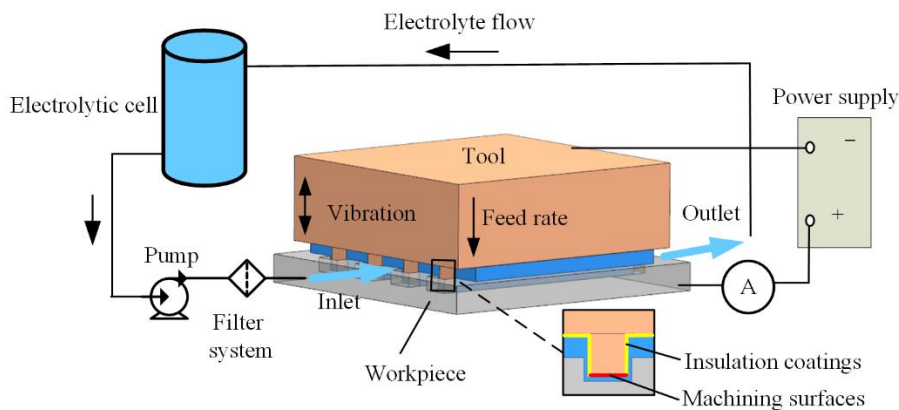


Figure 1. The schematic diagram of electrochemical machining the multiple slots

In ECM multiple slots of bipolar plates, the shape of tool cathode is usually constant cross-section structure. So the flow channels cross-section of inlet and outlet are equal. The cross-section of tool and flow channels is shown in Fig.1. Due to the electrolyte flows in the direction of slots length, the long and constant cross-section flow channels will cause the flow resistance increase and the electrolyte velocity decrease. Along the length of flow channels, the accumulation degree of metal hydroxide and other by-products is intensified gradually. As the electrolyte velocity decrease, it is difficult to remove the electrolysis products from the inter-electrode gap in time, especially in the end of the electrolyte flow channels. It will make the clogging in inter-electrode gap and lead to short circuit in processing. The distribution of electrolysis products in machining process with ordinary shaped cathode is shown in Fig.2. Although tool continuous feeding with low-frequency vibration can make the discharging capacity of electrolysis products enhance, the problems of electrolyte velocity decrease from long flow channels and constant cross-section are still difficult to solve. In order to improve the electrolyte flow velocity in inter-electrode gap, numerical simulations are carried out with ordinary flow channels. Then, a flow channels contraction cathode structure with variable cross-section is illustrated to improve the flow field distribution through simulations.

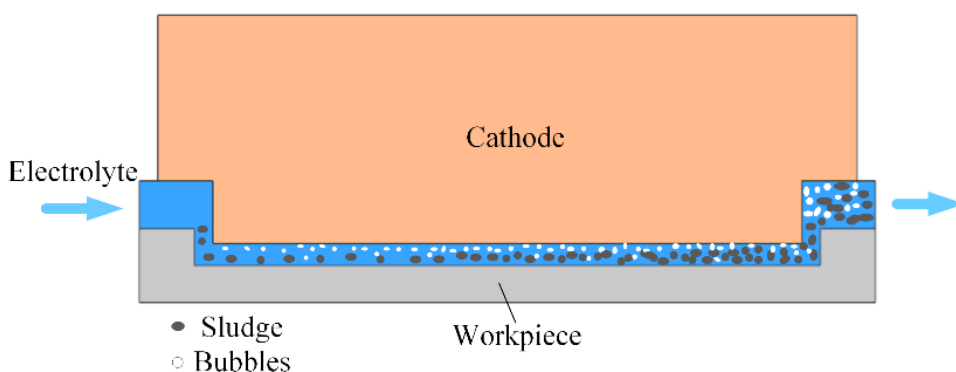


Figure 2. The schematic diagram of the machining process with ordinary cathode

3. NUMERICAL SIMULATIONS OF FLOW FIELD IN ECM

3.1 Finite element equations of electrolyte flow

During the ECM process, when the electrolyte reach to a turbulent state, the electrolysis products and bubbles in the inter-electrode gap can be taken away better. To ensure the electrolyte in a turbulent state, the Reynolds number should be greater than 2300. So, the electrolyte flow velocity satisfies the formula as follows [15]:

$$V > 2300\nu / D_h \tag{1}$$

Where V is the electrolyte flow velocity, ν is kinematic viscosity and D_h is hydraulic diameter.

The distribution of flow field in the inter-electrode gap is complex. Simulations will be conducted on the basic of two assumptions as follows.

(1) The liquid phase is incompressible, and metal hydroxide sludge in the electrolyte flow field is neglected.

(2) The flow motion of electrolyte obeys the momentum and mass conservation equations which can be written as

$$\frac{\partial U_i}{\partial x_i} = 0 \tag{2}$$

$$U_j \frac{\partial U_i}{\partial x_j} = -\frac{1}{\rho} \frac{\partial P}{\partial x_i} + \frac{\partial}{\partial x_j} \left(\nu \left(\frac{\partial U_i}{\partial x_j} + \frac{\partial U_j}{\partial x_i} \right) - \overline{u_i' u_j'} \right) \tag{3}$$

where U_i are the components of the mean velocity, x_i are the Cartesian coordinates, P is the mean electrolyte pressure, ρ is the electrolyte density, ν is the kinematic viscosity, and $-\overline{u_i' u_j'}$ is the Reynolds-stress tensor.

In this paper, the equation of the k - ε turbulent model [16-17] is used to analyze the flow field distribution, which can be written as:

$$\frac{\partial k}{\partial t} + U_j \frac{\partial k}{\partial x_j} = \frac{\partial}{\partial x_j} \left[\left(\nu + \frac{\nu_t}{\sigma_k} \right) \frac{\partial k}{\partial x_j} \right] + \nu_t \left(\frac{\partial U_i}{\partial x_j} + \frac{\partial U_j}{\partial x_i} \right) \frac{\partial U_i}{\partial x_j} - \varepsilon \tag{4}$$

$$\frac{\partial \varepsilon}{\partial t} + U_j \frac{\partial \varepsilon}{\partial x_j} = \frac{\partial}{\partial x_j} \left[\left(\nu + \frac{\nu_t}{\sigma_\varepsilon} \right) \frac{\partial \varepsilon}{\partial x_j} \right] + C_{\varepsilon 1} \frac{\varepsilon}{k} \nu_t \left(\frac{\partial U_i}{\partial x_j} + \frac{\partial U_j}{\partial x_i} \right) \frac{\partial U_i}{\partial x_j} - C_{\varepsilon 2} \frac{\varepsilon^2}{k} \tag{5}$$

The turbulence kinematic viscosity ν_t is determined as:

$$\nu_t = C_\mu \frac{k^2}{\varepsilon} \tag{6}$$

Where k is the turbulence kinetic energy, ε is the dissipation rate and t is the time. The values of the constants in the above formula are: $C_\mu=0.09$, $C_{\varepsilon 1}= 1.44$, $C_{\varepsilon 2}= 1.92$, $\sigma_k= 1.0$, $\sigma_\varepsilon= 1.314$.

3.2 Simulation of the ordinary flow channels with vibration

During the ECM multiple slots process, the constant cross-section flow channels are so long that make the insoluble byproducts and hydrogen bubbles block in inter-electrode gap sharply. This will cause the conductivity of electrolyte to decrease, which will make dissolving capacity of

electrolyte decrease and lead to short circuit in processing. So the tool continuous feeding composited with low-frequency vibration is usually adopted. It could improve the machining accuracy of ECM. In the literature, there are many relevant research about tool vibration during ECM processes. Natsu et al. improved both the processing speed and the machining accuracy through the application of the ultrasonic vibration to tool electrode [18]. Zhao et al. proposed a tool feed mode with vibration and enhanced the machining localization and stability [19]. Ebeid et al. achieved higher machining accuracy by correlating various machining parameters with low-frequency vibrations [20]. Reciprocating motion of the cathode can realize electrolyte pressure and velocity periodic variety in the inter-electrode gap, which are useful to renew the electrolyte and carry out electrolysis products in time. This result is in agreement with the reports by Hewidy [21] and Wang [22]. Hewidy et al. reported the effect of electrolyte pressure and tool vibration on the disposal of the electrolysis products in different cathode positions. Wang et al. analyzed tool vibration provides the positive effect on removal of electrolysis products and the renewal of electrolytic in the machining gap with time in a single vibration period.

The vibration equation of cathode is described as follows:

$$x_1 = A \sin(\omega_1 t + \varphi) \tag{7}$$

where A is the amplitude of cathode vibration, angular velocity $\omega_1=2\pi f$, f is the vibration frequency and φ is the phase angle.

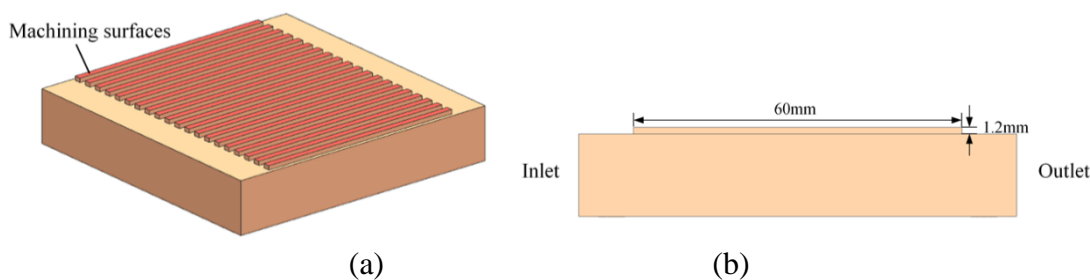


Figure 3. The ordinary shaped cathode model

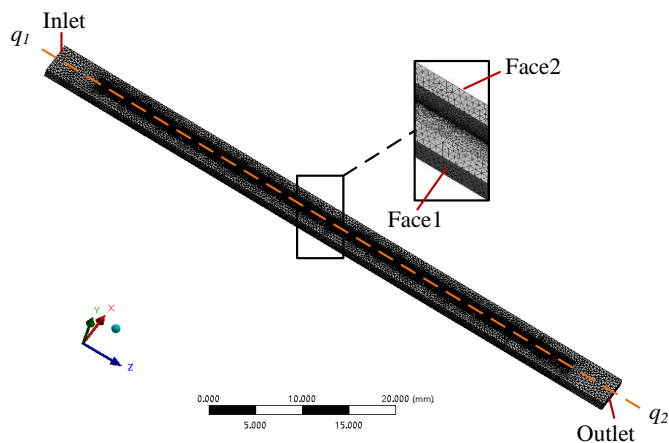


Figure 4. Flow model of one channel of ECM in the ordinary pattern

To get the distribution of electrolyte flow field with tool vibration, simulations of ordinary flow channels had been executed on the basic of standard $k-\epsilon$ turbulent model. It is assumed that the flow of electrolyte is approximately uniform in the inlet and outlet of electrolyte. Based on a model of bipolar plates parts, the ordinary cathode model with constant cross-section structure is shown in Fig.3. It has 20 cuboids in the cathode surface, the length, the width and the height are 60mm, 1.9mm and 1.2mm, respectively.

In this investigation, the amplitude of cathode vibration is 0.3mm and the vibration frequency f is 10Hz. The minimum and maximum inter-electrode gap are 0.1mm and 0.7mm, respectively. As shown in Fig.4, the flow model of one slot and the specific dynamic mesh setting are carried out. The face1 and face2 are periodic boundary and the electrolyte inlet and outlet are pressure boundary. The cross-sectional line q_1q_2 is in the xz plane. Based on our preliminary work, the electrolyte pressure of inlet and outlet are 0.8 MPa and 0.1 MPa [14], respectively.

The electrolyte velocity distribution with ordinary channels along q_1q_2 is shown in Fig.5. The contours of 8 inter-electrode gaps, 0.612mm, 0.4mm, 0.188mm, 0.1mm, 0.188mm, 0.4mm, 0.612mm and 0.7mm, were selected in one period. When the inter-electrode gap is less than or equal to 0.188mm, the circuit turned on.



Figure 5. The velocity contours of different gap with ordinary cathode

As shown in Fig.5, the electrolyte velocity increase with the increase of inter-electrode gap. With the current turned on periodically, the electrolysis products accumulates gradually in the inter-electrode gap especially in the end of the electrolyte flow channels. However, the electrolyte flow velocity from 7.1m/s to 4.7m/s in the inlet and outlet of flow channel respectively when the inter-electrode gap at 0.1mm. The electrolyte flow velocity in flow channel outlet is too slow to remove the electrolysis products in time. To a large extent, dimensional accuracy and the processing stability will decrease for this reason. And even, a short circuit may be happen that will damage to the workpiece and cathode. The results of simulation analysis shows that the tool vibration still can't solve the electrolyte field problem which causes by the long and constant cross-section flow channels.

3.3 Simulation of the new contraction flow channels with vibration

Based on the above analysis, the long and constant cross-section flow channels will leads to the attenuation of electrolyte velocity and short circuit. To eliminate this problem, a flow channels contraction cathode structure with variable cross-section is illustrated. Therefore, the constant cross-section of flow channels are converted into convergent cross-section which will enhance the back pressure of the electrolyte and electrolyte velocity in the outlet. The acceleration effect of electrolyte can improve process stability and relieve accumulation of electrolysis products along the flow path, especially in the outlet of electrolyte.

The morphology of flow channels contraction cathode model is shown in Fig.6 (a). Viewed from the cross-section (Fig.6 b), the area of electrolyte inlet will increase with the growth of H value on the basis of the ordinary cathode.

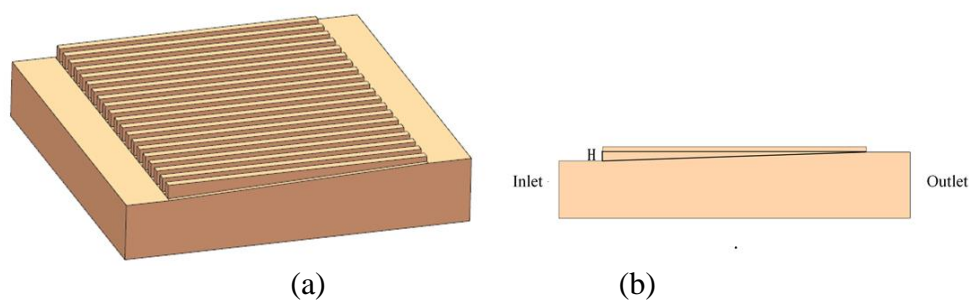


Figure 6. The flow channels contraction cathode model

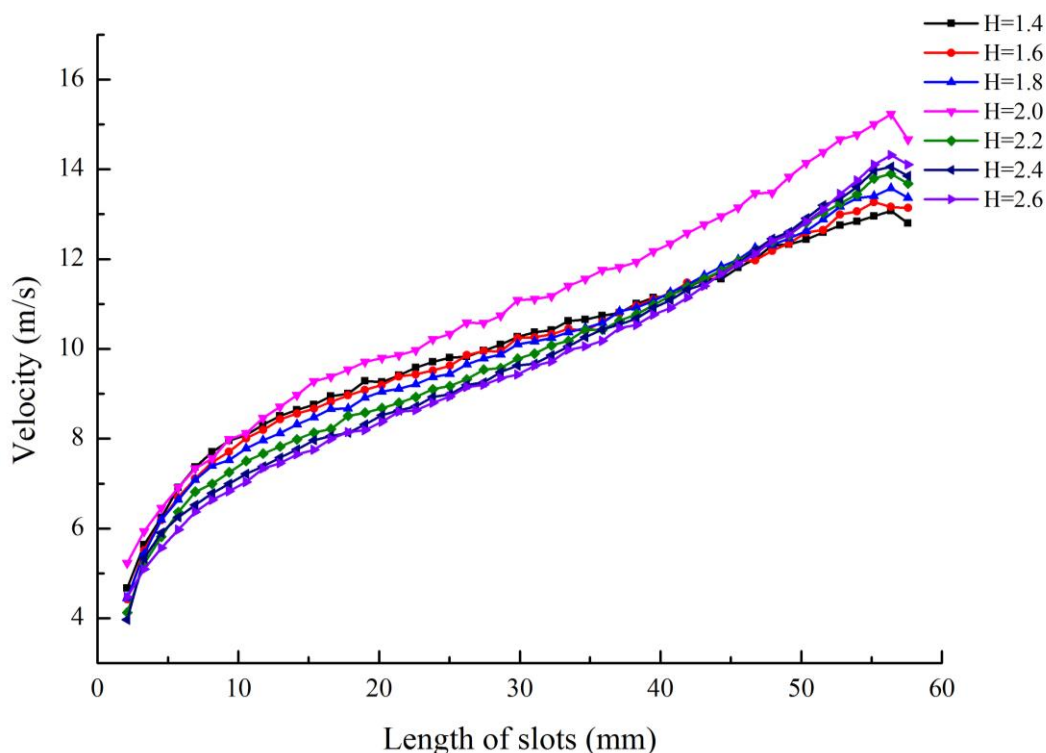


Figure 7. The electrolyte velocity curves with different H value along length of slots

To observe the variations of flow field through using different H value, the velocity distribution of electrolyte along the length of slots in the inter-electrode gap of 0.7mm are operated in Fig. 7. The inter-electrode gap of 0.7mm is the maximum inter-electrode gap in one period, which represents the maximum of electrolyte flow velocity during the whole machining process. High flow velocity in the non-machining time has a beneficial effect on the update of electrolyte.

As Fig. 7 shows, the electrolyte velocity have same trend with different H value. They are all vary from low to high velocity. However, when H value is 2mm, the flow velocity of electrolyte in the inter-electrode gap is higher than others obviously. So, H value has been determined.

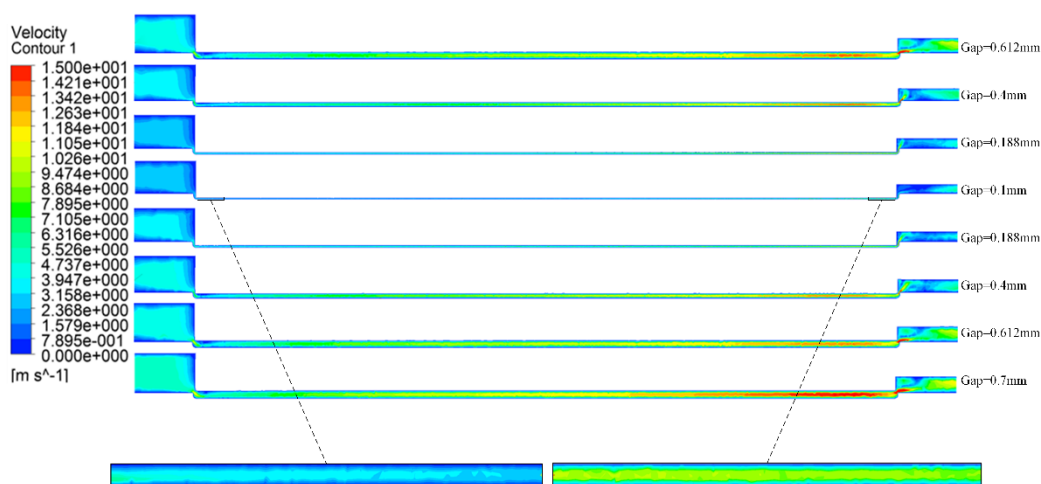


Figure 8. The velocity contours of different gap with flow channels contraction cathode

The electrolyte velocity distribution of different gaps with flow channels contraction cathode is shown in Fig.8. The contours of 8 inter-electrode gaps were also selected in one period to show the variations of electrolyte velocity. The electrolyte flow velocity are increasing gradually from the electrolyte inlet to the outlet at various gaps, which is contrary to the electrolyte velocity variation with the ordinary cathode. When the inter-electrode gap is 0.1mm, namely, the nearest gap between the cathode and the workpiece, the electrolyte flow velocity in the inter-electrode gap is increased from 3.9m/s to 9.4m/s which is the ideal velocity changes.

The electrolyte velocity with the flow channels contraction cathode is lower than that with the ordinary cathode in the inlet of electrolyte, but there is a small amount of insoluble byproducts. And large numbers of the insoluble byproducts will gather in the outlet of electrolyte, they can be taken away by the higher electrolyte velocity when using the flow channels contraction cathode. Therefore, the simulations results show that the flow channels contraction cathode is more suitable than the ordinary cathode for the production of long slots.

4. EXPERIMENTS AND DISCUSSION

In order to testify the stability of flow channels contraction cathode, some comparison experiments were executed with the ordinary and flow channels contraction cathode under the

condition of vibration. The ECM fixture of multiple slots and some important components in the machining process are demonstrated in Fig.9. The clamping fixture is made of epoxy materials which has small deformation rate and good size stability. The cathode and workpiece are all made of SS304 stainless steel.

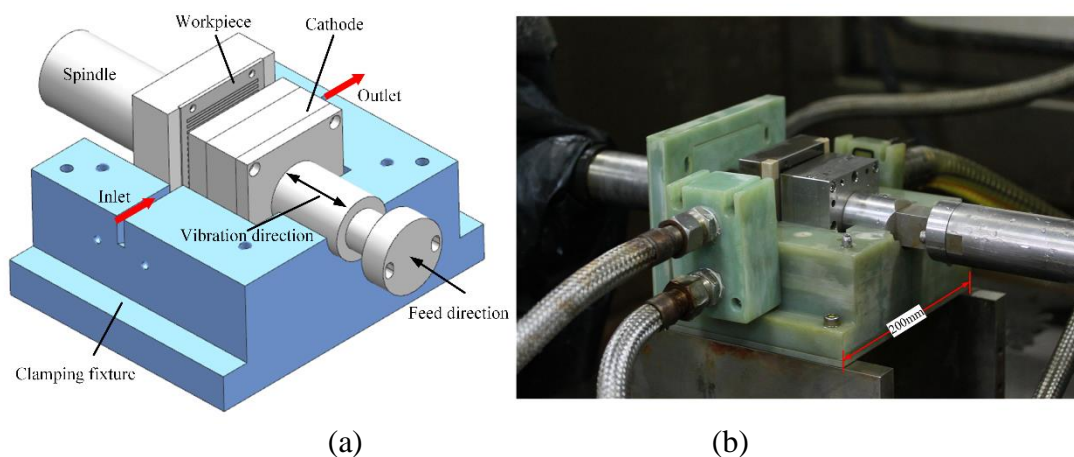


Figure 9. The ECM fixture and important components (a) model (b) real object

The ECM experimental conditions and parameters are shown in Table1. The time of one period is 0.1s because the vibration frequency f is 10Hz. A vibration period of 0.1s consists of machining time and non-machining time. The machining time means the time of circuit breakover when the inter-electrode gap is less than the effective gap between cathode and workpiece. The proportion of the machining time to one period can be seen in Fig.10. The proportion of the machining time to one period is 25%, so the duty cycle is 25%.

Table 1. ECM experimental conditions and parameters

conditions	value
Electrolyte	20%NaNO ₃
Voltage	20V
Electrolyte inlet pressure	0.8MPa
Electrolyte outlet pressure	0.1MPa
Temperature of electrolyte	30±1 °C

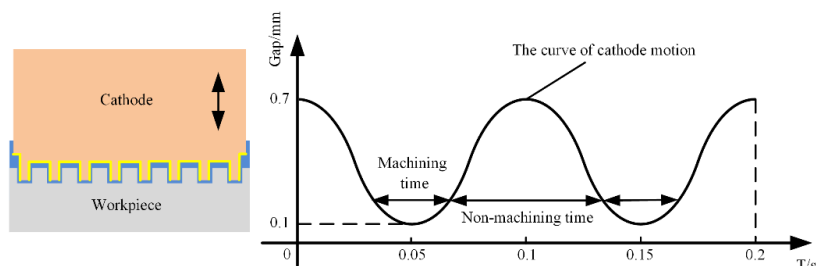


Figure 10. The proportion of the machining time to one period

Under the same machining parameters, feed rate comparison experiments with different cathodes were conducted. Firstly, the ordinary cathode was adopted. When the feed rate is 0.05mm/min, the machining process could go smoothly. However, with the feed rate increased to 0.06mm/min, the short circuit happened in the outlet of the workpiece. The workpiece with short circuit is shown in Fig.11 (a). Secondly, experimental tests carried out with the flow channels contraction cathode. Multiple slots were machined with different feed rate which starts from 0.05mm/min. The experiments could be conducted as normal when the feed rate reached 0.1mm/min and the machined workpiece is shown in Fig.11 (b). However, the short circuit happened when the feed rate was 0.11mm/min. Compared with the ordinary cathode, the feed rate of the flow channels contraction cathode could increase by 100%. As shown in Fig.12, the local three dimension surface images were measured with a digital microscope (VHX-5000, Keyence, Japan).

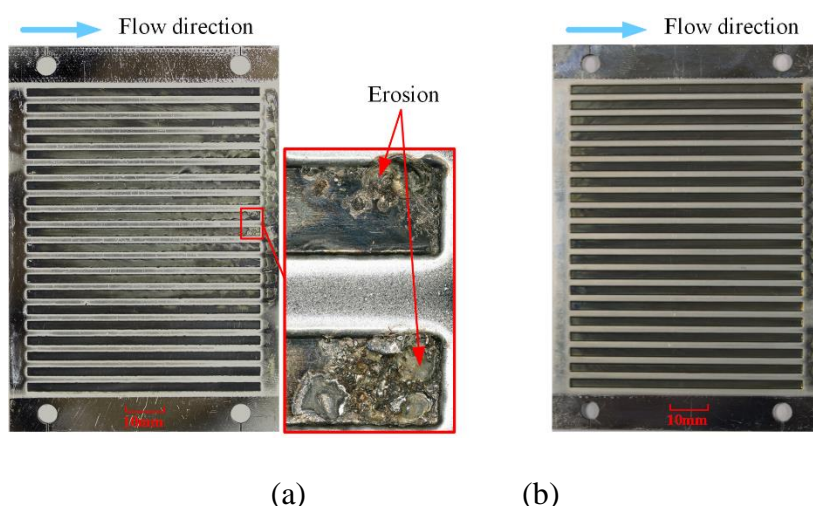


Figure 11. The workpiece with different cathode and feed rate, (a) Ordinary cathode, feed rate 0.06 mm/min (b) flow channels contraction cathode, feed rate 0.1 mm/min

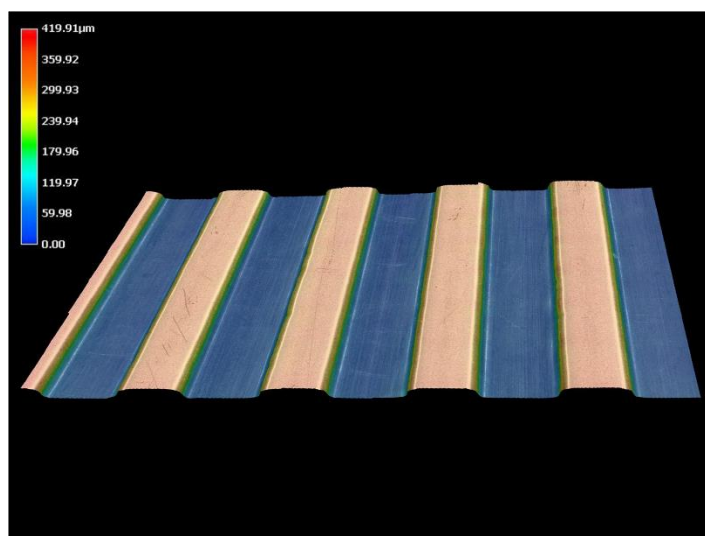


Figure 12. Local three dimension surface images

The depth of multiple slots which is fabricated by the flow channels contraction cathode has been measured by using a profile meter (DVM 5000, Leica, Germany). As shown in Fig.13, the measuring positions are located in the intersection of red line and green line. The depth values are shown in Fig.14. The maximum and minimum depths of all measuring positions are 324.2 μm and 271.1 μm respectively, which means that the depth of machined workpiece is $300\pm 30\mu\text{m}$. The experimental results show that using the flow channels contraction cathode is able to improve the flow field and fabricate multiple slots with good depth uniformity. This result is agreed with the report by Rajurkar et al. [23], which improved machining accuracy and uniformity through reducing the flow field disrupting phenomena. Under the condition of vibration, the flow channels contraction cathode makes good effect on renewing electrolyte and making conductivity uniform, which can improve the machining efficiency greatly and ensure the uniformity of depth.

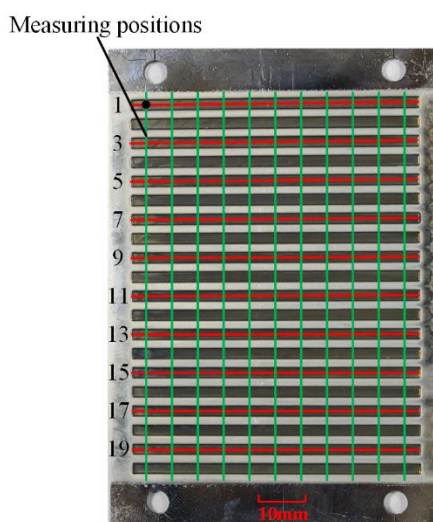


Figure 13. Measuring positions with flow channels contraction cathode

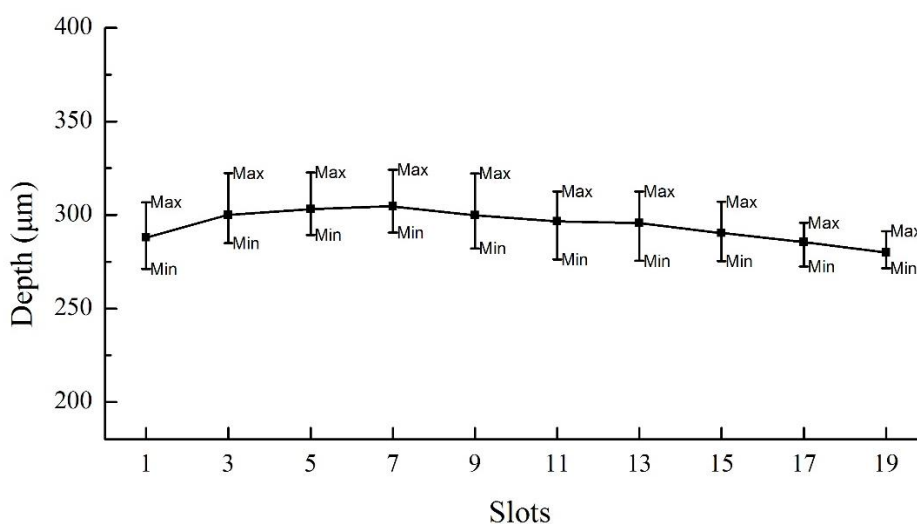


Figure 14. Depth of multiple slots machined with ECM process

5. CONCLUSION

Due to the electrolyte flows in the direction of slots length, the long and constant cross-section flow channels will make the electrolyte velocity decrease and electrolysis products accumulate in the outlet of electrolyte. In spite of adopting vibration, the machining effect with the ordinary cathode is still not optimistic. Therefore, a different cathode structure is proposed which can enhance the stability of process and take away electrolysis products effectively. The following conclusions can be reached on the basis of simulations and experiments:

- (1) The flow channels contraction cathode structure with variable cross-section is proposed through numerical simulations. And the final model parameter is determined.
- (2) Under the same machining parameters, the maximum feed rate of flow channels contraction cathode doubles that of ordinary cathode.
- (3) A bipolar plate with depth of $300\pm 30\mu\text{m}$ and length of 60mm is fabricated on a stainless steel sheet.

ACKNOWLEDGEMENTS

This article was sponsored by the China Natural Science Foundation (51405230).

References

1. R.F. Silva, D. Franchi, A. Leone, L. Pilloni, A. Masci, A. Pozio, *Electrochim. Acta*, 51 (2006) 3592.
2. R. Taherian, *J. Power Sources*, 265 (2014) 370.
3. S. Karimi, N. Fraser, B. Roberts, F.R. Foulkes, *Adv. Mater. Sci. Eng.*, 2012 (2012) 1.
4. J.C. Hung, C.C. Lin, *J. Power Sources*, 206 (2012) 179.
5. T.C. Chen, J.M. Ye, *Int. J. Adv. Manuf. Tech.*, 64 (2013) 1365.
6. C.K. Jin, C.G. Kang, *J. Power Sources*, 196 (2011) 8241.
7. K.P. Rajurkar, D. Zhu, J.A. McGeough, J. Kozak, A. De Silva, *CIRP Ann. – Manuf. Techn.*, 48 (1999) 567.
8. W. Natsu, T. Ikeda, M. Kunieda, *Precis. Eng.*, 31 (2007) 33.
9. C.C. Chen, J.Z. Li, S.C. Zhan, Z.Y. Yu, W.J. Xu, Study of Micro Groove Machining by Micro ECM, 18th CIRP Conference on Electro Physical and Chemical Machining (ISEM), Tokyo, Japan, 2016, 418-422.
10. B. Ghoshal, B. Bhattacharyya, *Int. J. Mach. Tool. Manu.*, 64 (2013) 49.
11. C. Madore, O. Piotrowski, D. Landolt, *J. Electrochem. Soc.*, 146 (1999) 2526.
12. S.J. Lee, C.Y. Lee, K.T. Yang, F.H. Kuan, P.H. Lai, *J. Power Sources*, 185 (2008) 1115.
13. G.X. Liu, Y.J. Zhang, Y. Deng, H.Y. Wei, C. Zhou, J.W. Liu, H.P. Luo, *Int. J. Adv. Manuf. Tech.*, 89 (2016) 407.
14. J. Liu, X.C. Jiang, D. Zhu, Electrochemical machining of multiple slots with low-frequency tool vibrations, 18th CIRP Conference on Electro Physical and Chemical Machining (ISEM), Tokyo, Japan, 2016, 799-803.
15. D. Zhu, J.C. Zhang, K.L. Zhang, J. Liu, Z. Chen, N.S. Qu, *Int. J. Adv. Manuf. Technol.*, 80(2015) 637.
16. N. Koutsourakis, J.G. Bartzis, N.C. Markatos, *Environ. Fluid Mech.*, 12 (2012) 379.
17. F. Juretić, H. Kozmar, *J. Wind Eng. Ind. Aerod.*, 115 (2013) 112.
18. W. Natsu, H. Nakayama, Z.Y. Yu, *Int. J. Precis. Eng. Man.*, 13 (2012) 1131.
19. J.S. Zhao, X.L. Zhang, Z.W. Yang, Y.M. Lü, Y.F. He, *Int. J. Adv. Manuf. Technol.*, 91 (2016) 1.

20. S.J. Ebeid, M.S. Hewidy, T.A. El-Taweel, A.H. Youssef, *J. Mater. Process. Tech.*, 149 (2004) 432.
21. M.S. Hewidy, S.J. Ebeid, T.A. El-Taweel, A.H. Youssef, *J. Mater. Process. Tech.*, 189 (2007) 466.
22. F. Wang, J.S. Zhao, X.L. Zhao, Z.W. Yang, W.M. Gan, Z.J. Tian, *Int. J. Adv. Manuf. Technol.*, 90 (2017) 971.
23. K.P. Rajurkar, D. Zhu, *CIRP Ann. – Manuf. Techn.*, 48 (1999) 139.

© 2018 The Authors. Published by ESG (www.electrochemsci.org). This article is an open access article distributed under the terms and conditions of the Creative Commons Attribution license (<http://creativecommons.org/licenses/by/4.0/>).